THIN-FILM INTRACORTICAL RECORDING MICROELECTRODES

Quarterly Report #11

(Contract NIH-NINDS-NO1-NS-7-2364)

October-December 1999

Submitted to the

Neural Prosthesis Program
National Institute of Neurological Disorders and Stroke
National Institutes of Health

by the

Center for Integrated MicroSystems
Department of Electrical Engineering and Computer Science
University of Michigan
Ann Arbor, Michigan
48109-2122

January 2000

Thin-Film Intracortical Recording Microelectrodes

Summary

The goal of this contract has been to develop a family of active recording probes suitable for fundamental studies in neurophysiology and for use in neural prostheses. The probes have 64 sites, of which eight can be selected for simultaneous use by the external world. On one of the probe designs (PIA-2B/3B), the neural signals are buffered and then passed directly off chip, whereas on the other (PIA-2/-3) the signals are amplified, multiplexed, and then passed off chip to minimize external leads. Both two-dimensional (2D) and three-dimensional (3D) versions of these probes are being developed.

During the past term, we have continued to fabricate additional passive probes for use by a variety of investigators. This has included processing additional wafers of our standard probe designs as well as designing two new mask sets of custom designs. The second of these will employ 1.5μm features, shrinking current dimensions by a factor of two. We have also implanted passive probes in guinea pig inferior colliculus and auditory cortex using normal and side-mounted recording sites. The standard sites have typically recorded for about one month, while the side-mounted sites are still recording after three weeks as of this writing. We expect the side-mounted sites to do better since micromovements there will tend to clear the sites of protein buildup that is hypothesized to mask recorded units from the site surface. We have found that by inducing brain movement by hyperventilating the animals successfully and repeatedly restores recording ability. This will be explored further. Polypyrrole is being explored as a recording site material because this polymer can be doped to prevent the adhesion of protein on its surface. These sites are low in impedance but have experienced some adhesion problems which are being addressed. We hope to have longer-term recording experiments with polyprrole to report by the end of the coming quarter. We have also developed improved cleaning procedures for use on probes destined for chronic use. Experiments in a culture medium with bovine serum have shown that without the new cleaning procedures, adverse cell reactions and cell death in the immediate vicinity of the probe surface sometimes occur.

A series of passive probes have been designed to allow a direct comparison with microwire electrodes and are now being fabricated. The design of our non-multiplexed active recording probe, PIA-2B, is now being iterated to upgrade its switches and recording buffers. A resistor technology based on ion-implanted polysilicon has been developed to allow simple resistive input clamps to be used to stabilize the input bias of the preamplifiers by loading down the electrochemical cell formed at the recording site. As presented previously, we require an input dc resistance between about 75MΩ and 500MΩ in order to achieve proper stability in the face of both battery offsets and optically-based current generation. The resistor technology allows a sheet resistance of 35MΩ/square to be achieved, so that such resistances would require very little area at the preamplifier inputs and would stabilize the input dc levels to better than 1mV in the face of several hundred millivolt offsets. Finally, we are continuing to refine designs for closed-loop preamplifiers and for the various circuits required for the realization of a telemetry-based probe interface. We hope to include the new preamplifiers on the modified version of PIA-2B as well as on a redesigned version of PIA-2/-3 that is now in development.

Thin-Film Intracortical Recording Microelectrodes

1. Introduction

The goal of this program is the realization of batch-fabricated recording electrode arrays capable of accurately sampling single-unit neural activity throughout of volume of cortical tissue on a chronic basis. Such arrays will constitute an important advance in instrumentation for the study of information processing in neural structures and should also be valuable for a number of next-generation closed-loop neural prostheses, where stimuli must be conditioned on the response of the physiological system.

The approach taken in this research involves the use of solid-state process technology to realize probes in which a precisely-etched silicon substrate supports an array of thin-film conductors insulated above and below by deposited dielectrics. Openings in the dielectrics, produced using photolithography, form recording sites which permit recording from single neurons on a highly-selective basis. The fabrication processes for both passive and active (containing signal processing circuitry) probe structures have been reported in the past along with scaling limits and the results of numerous acute experiments using passive probes in animals. In moving to chronic implant applications, the major problems are associated with the preserving the viability of the sites in-vivo (preventing tissue encapsulation of the sites) and with the probe output leads, both in terms of their number and their insulation. The probe must float in the tissue with minimal tethering forces, limiting the number of leads to a few at most. The encapsulation of these leads must offer adequate protection for the meg-ohm impedance levels of the sites while maintaining lead flexibility.

Our solution to the lead problem has involved two steps. The first has been to embed circuitry in the probe substrate to amplify and buffer the signals and to multiplex them onto a common output line. Using this approach, signal levels are increased by factors of over 100, impedance levels are reduced by four orders of magnitude, and the probe requires only three leads for operation, independent of the number of recording sites. A high-yield merged process permitting the integration of CMOS circuitry on the probe has been developed, and this circuitry has been designed and characterized. The second step has involved the development of silicon-based ribbon cables, realized using the same probe technology, to conduct the neural signals to the outside world. These cables have shown significant advantages over discrete leads, both in terms of the ease with which chronic implants can be assembled and in terms of the ability of the cables to survive long-term biased soaks in saline. The cables can be built directly into the probes so that they come off of the wafer as a single unit, requiring no joining or bonding operations between them. The cables are also significantly more flexible than previously-used discrete wire interconnects.

This contract calls for the development of active probes for neural recording. A 64-site 8-channel probe with site selection and signal buffering but no multiplexing has been developed (PIA-2B) along with a high-end multiplexed probe that includes gain (PIA-2). During the past quarter: 1) we have continued to fabricate passive probes for a variety of users; 2) we have continued to explore the use of polypyrrole recording sites and have examined our cleaning procedures for chronic use; 3) we are developing a new set of passive probes to better understand their chronic recording viability; 4) we have developed a shunt resistor technology for input bias stabilization; 5) we have continued to refine circuitry for leadless probe operation; and 6) we are developing a new amplifier design for

use with two- and three-dimensional active recording probes. Work in these areas is discussed in the following sections.

2. Passive Probe Developments

During the past quarter, three additional wafers from the STANDARDS mask set were completed with iridium sites. While probes from this mask set continue to satisfy the needs of most Center for Neural Communication Technology (CNCT) users, the resource Center continues to get requests from users with special preparations that require custom designs. Design and layout for two new passive probe mask sets is currently underway and fabrication should commence in the coming quarter.

The first mask uses standard design rules and includes designs for Charles Miller and Paul Abbas of the University of Iowa for recording from the VIII nerve of the cat; Sandy Bledsoe of the University of Michigan for recording and stimulation in the guinea pig IC, David Edell of InnerSea Technology for interfacing between various devices and for testing encapsulation; Christophe Pouzat and Leslie Kay of Caltech for recording from olfactory bulb in the rat; Mark Knuepfer for recording from regenerated sympathetic nerve in rat; and Wayne Aldridge of the University of Michigan for recording from output structures of the rat basal ganglia.

The second mask set will incorporate smaller minimum features (1.5µm as opposed to the standard 3µm) to realize higher density, single-shank probes. While these feature sizes are not small by industrial standards, they will present a challenge in our own laboratory. The designs were submitted by CNCT collaborators Phil Hetherington, Tim Blanche and Nicholas Swindale of the University of British Columbia for 3-D cell localization and 2-D current source density analysis in cortex. These probes will have up to 64 sites on a single shank arranged in two or three staggered rows on a substrate that is less than 250µm wide.

3. Chronic Recording with Passive Thin-Film Microprobes

Chronic Animals

During this past quarter, we have implanted four animals with chronic devices; the first (Turk) was a Brain-in-the-Box(BIB)-type electrode placed into the cerebellum instead of auditory cortex. We had been having difficulties recording for extended time periods with the BIB electrodes in auditory cortex and wanted to see if this was due to the electrode design or a peculiarity of our target tissue. For this initial attempt we have seen no difference in the length of time recordings can be sustained (approximately 3 weeks). The second implant (Bing) was a 4-shank electrode in inferior colliculus (IC). For this animal we tried using TiN for the recording sites to see if the greater surface area and lower impedance of this site material would help the electrode become better integrated within the neural tissue; this animal responded for approximately 4 weeks. The impedances for both implants remained within good levels (less than 8MΩ at 1kHz). The next two implants (Bang and Plug) were single-shank electrodes with sites along the edge (Gil Case design). Our thought was that by having sites along the edge, there would be more movement within the tissue to help prevent encapsulation and thus the implants might record neurons for longer time periods. These animals have been implanted in IC for 2 and 3 weeks and are still recording neurons. The first of these two implants moved during closure and is not in IC anymore but has a nice spontaneous unit on one of the channels.

Rejuvenation

Sandy Bledsoe, of the Center for Neural Communications Technology (CNCT), recommended a new rejuvenation technique, which consists of hyperventilating the guinea pig. His thought was that by causing rapid breathing, the brain would pulsate more within the cranium and perhaps cause the electrode to move slightly and free itself of any encapsulation! We did this for both Turk and Bing, which had both stopped responding; we got a noticeable improvement in recordings for Turk, but not for Bing. We think that this may be due to the target tissue, Turk's electrode is placed within a surface structure (cerebellum) and Bing's within a deeper structure (IC); so there might be more movement at the surface compared to the deeper location. This new rejuvenation procedure has been tried successfully four times on Turk, which is still recording nicely. Figure1 shows pre- and post-rejuvenation impedances for Turk. Most channels showed a reduction in impedance, although three channels increased in impedance, two of which had extremely low impedances to start with. Figure 2 shows pre- and post-rejuvenation spontaneous neural recordings for Channel 5, which showed the most noticeable improvement in recording quality. Another technique, suggested by David J. Anderson, is to try negative instead of positive pressure, which may cause less stress on the animal. We have not yet tried this but will with another animal.

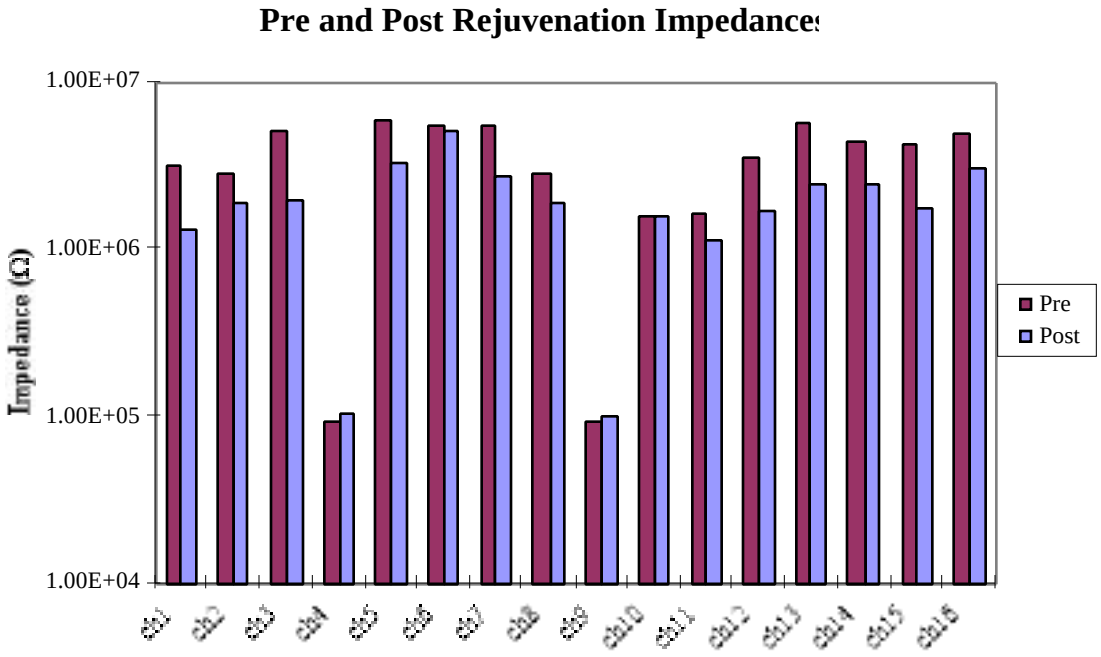

Fig. 1: Pre- and post-rejuvenation impedances for each of the 16 sites. Most sites showed a decrease in impedance after rejuvenation.

Polypyrrole

In the previous quarter, we had reported on the collaboration with Dave Martin and Xinyan Cui from the Material Science Department, coating iridium sites with polypyrrole to increase the surface area and perhaps extend the recording period of chronically implanted animals. After several weeks, the electrodes stopped recording neural activity so the

animals were euthanized. The electrodes were explanted and examined using scanning electron microscopy (SEM). We discovered that the polypyrrole had come off of the iridium sites (Fig. 3). To improve the biocompatibility of the neural probe and provide more intimate contact between the electrode site and the biological tissue, we have successfully deposited a bioadhesive polymer (SLPF) together with polypyrrole using an electrochemical deposition. Gold rather than iridium sites have been used because of the inertness of the element and the smoothness of the surface, which removes having to first do electrochemical and morphological characterizations. The resulting coating has a rough fibrous morphology which provides higher interfacial area at the electrode sites and high

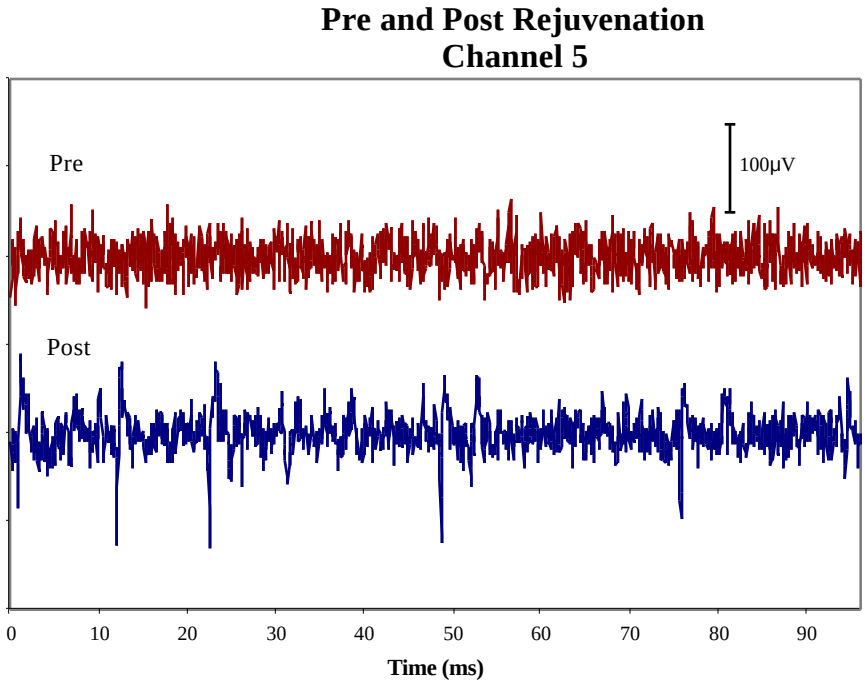

Fig. 2: Pre-and post-rejuvenation recordings for site 5.

density of RGD sequence to promote cell adhesion (Fig. 4).

To ensure that the deposition of conducting polymer/biopolymer film will not sacrifice the electrical properties of the gold electrode, impedance spectroscopy (IS) was measured (Figs. 5 and 6). From the impedance spectroscopy we can see that after coating the sites with polypyrrole/SLPF, the IS of the electrode has changed dramatically. Bare gold sites have an almost purely capacitive impedance behavior (indicated by the high constant phase angle of 80° between 10Hz and 10,000Hz), which is mainly due to the extremely smooth surface of gold. At the mean frequency of neural activity (1kHz), the magnitude of the impedance is as high as 370kΩ (for a 4000µm^2 site). After coating with PPy/SLPF, the phase angle of the electrode decreased 50-70% over a wide frequency range. The magnitude of the impedance decreased to 90kΩ at 1kHz. In other words, the impedance of the electrode became much more resistive after being modified with the conducting polymer/biopolymer. Two reasons might explain this interesting phenomenon: 1) the morphology of the coating is rough and sometimes fibrous, which increases the surface area of the electrode; 2) the conducting polymer can undergo a reversible redox reaction under the appropriate potential change, which provides a high charge capacity to the electrode.

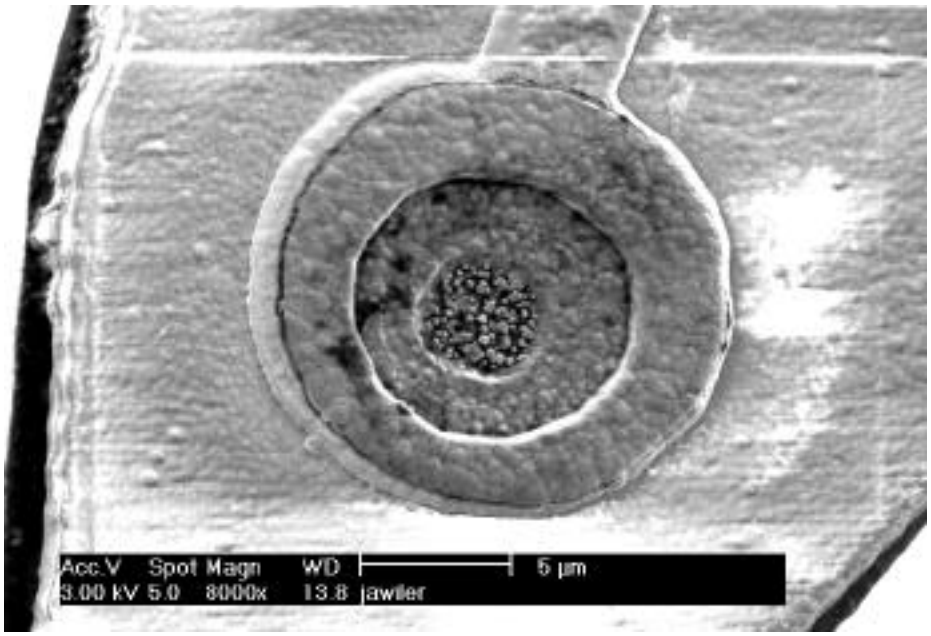

Fig. 3: Scanning electron micrograph of a once-polypyrrole-coated iridium site, implanted in guinea pig IC for 66 days. There is no evidence of any remaining polypyrrole.

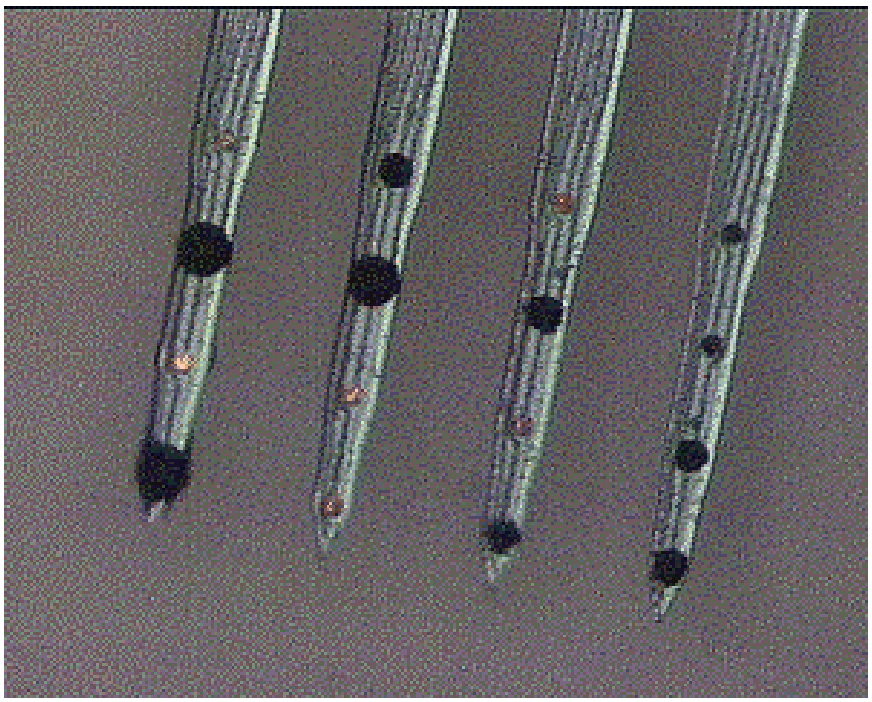

Fig. 4: Light microcopy image of gold sites, some coated with polypyrrole (black sites) of various thicknesses.

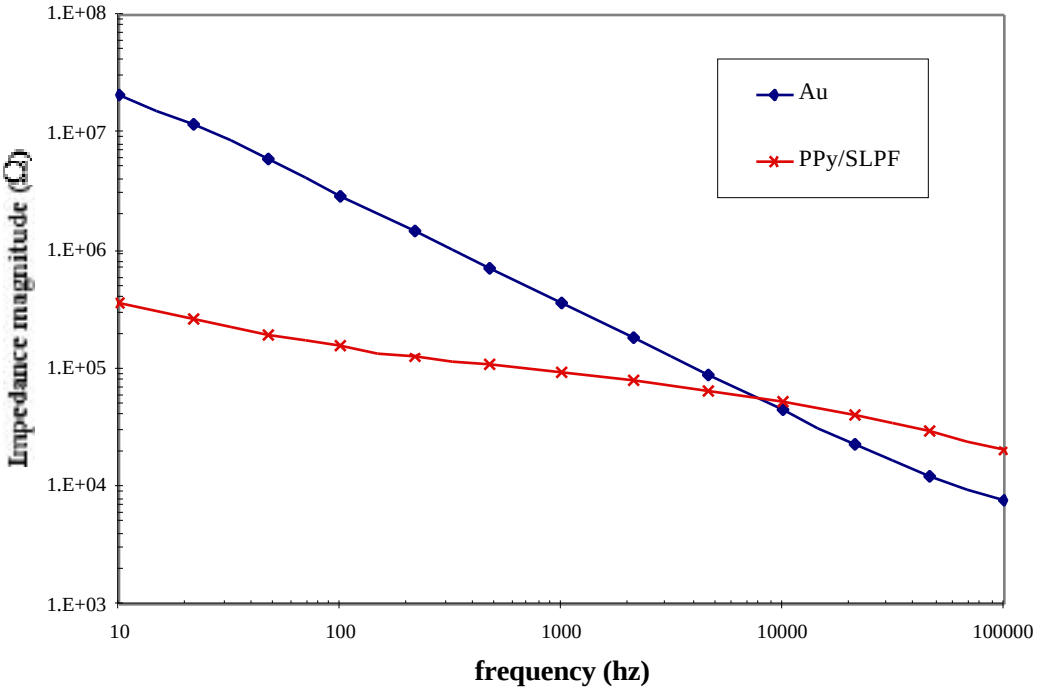

Fig. 5: Impedance magnitude vs. frequency for bare gold and coated gold sites.

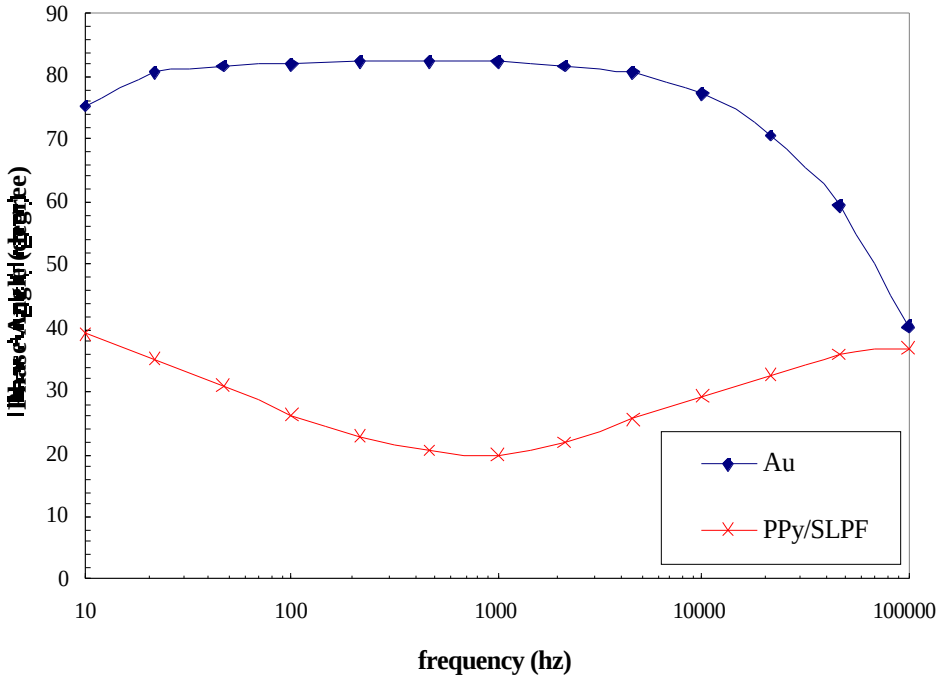

Fig. 6: Phase angle vs. frequency for bare gold and coated gold sites.

The following cyclic voltammagram (CV) data demonstrates this behavior (Fig. 7). PPy/SLPF-1 and PPy/SLPF-2 are the same material but deposited in different amounts. The more charge passed through during the electrochemical deposition, the more film is deposited on the site, consequently the higher charge capacity indicated by the area of the CV curve.

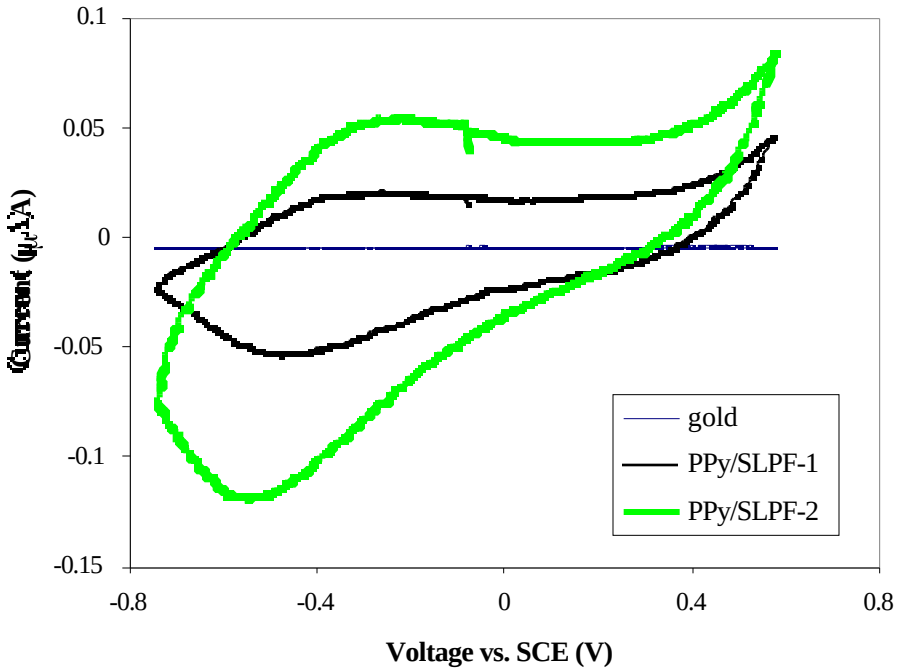

Fig. 7: Cyclic voltammagrams for bare gold and polypyrrole coated sites.

Electrode Cleaning

One issue that we have been concerned with for a long time, and one which may ultimately effect our chronic recordings, is that of cleanliness. We do clean the electrodes after they come out of the EDP release etch with a solvent cleaning sequence, which includes multiple rinsing in warm acetone, isopropyl alcohol and deionized water. But we have long thought that we should perhaps be doing something more. In an attempt to examine how well the electrodes are cleaned of their processing chemicals, one of the CNCT post-doctoral students, Valerie Lee, placed our normally-cleaned probes (untreated) and extra-cleaned probes in Dulbecco's Modified Eagle culture medium with 10% Fetal Bovine Serum. The extra cleaning procedure is a combination of basic and acidic solutions as follows:

- Ammonium hydroxide, 30% hydrogen peroxide, water (1:1:5), 5 min. or 20 min. at 80°C
- Rinse with deionized water, hydrochloric acid, 30% hydrogen peroxide, water (1:1:5), 5 min. or 20 min. at 80°C,
- Rinse with deionized water.

Probes were cleaned in both of the above ways (5 and 20 min.) or were left untreated. One-third of untreated probes (no extra cleaning) showed patchy cell surface growth only and cell death in the surrounding culture medium. All treated (extra cleaned) probes resulted in complete surface coverage by cells contiguous with cells in the medium, indicating an apparent benefit of the extra cleaning procedure (Fig. 8). Studies of the effects of the cleaning procedures on probe electrical characteristics (impedance spectroscopy) and structural integrity (SEM) are underway and will be reported on in subsequent quarterly reports.

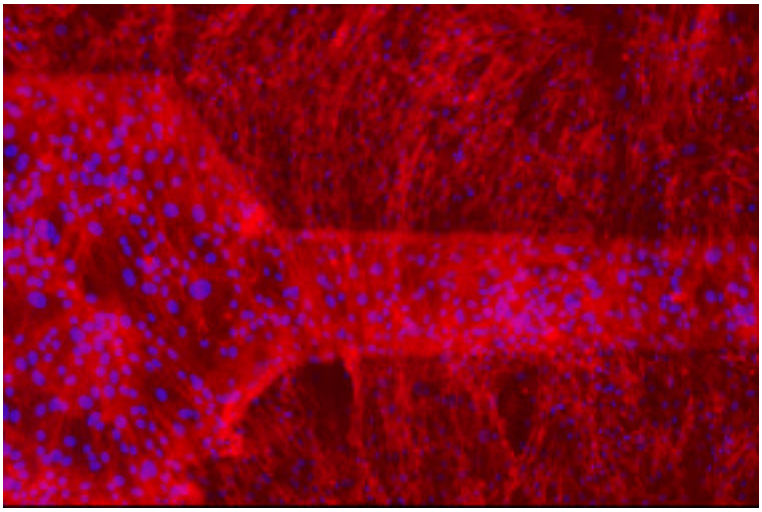

Fig. 8: Light microscopy image showing actin filaments (red) and nuclei (blue) after a 20-minute cleaning.

4. Development of a 64-Site Eight-Channel Non-Multiplexed Recording Probe (PIA-2B)

During the past quarter, work has progressed on the redesign of a 64-site front-end-selected and buffered probe. The design and architecture of this probe have already been reported, and the probe fabrication demonstrated the success of improvements to the active probe process: the fabricated probes showed good backside circuit protection, no aluminum hillocking or LTO adhesion problems, and good circuit and site contacts. All digital and analog circuit blocks on the probe function as designed; however a processing error led to unacceptable levels of interchannel crosstalk. In addition, some areas for improvement and design modification have been identified during testing of the probe.

As reported last quarter, high resistance polysilicon streamers in the "shadow" of the step between the circuit area and the probe bodies resulted from the conformal nature of the polysilicon film and the anisotropic nature of the poly etch. This problem will be addressed in future runs in several ways. First of all, a test structure is being added to the mask set which will allow the wafers to be tested after the Reactive Ion Etch (RIE) process to verify that all poly in the "shadow" the active area step has been removed. In addition, one patterned "monitor" wafer will be placed in the RIE during *each* poly etch. This will allow the etch rate to be monitored accurately using spectrophotometer (SP) measurements. Without a monitor wafer this is not possible, since the various thin films underneath the polysilicon being patterned prevent an accurate measurement of the film thickness as the

etch progresses. Using the monitor wafer, we will aim for an overetch of the polysilicon on the order of 10%, which will provide a healthy safety margin, ensuring that the polysilicon is completely etched without adversely affecting the length of the polysilicon gates in the circuit area. The drawback to using a monitor in each run is the resulting increase in process time (both for additional lithography and etch time); however, in light of the large run-to-run variations in etch rate and the lack of etch endpoint detection, this is a good tradeoff.

In the course of testing, it was also discovered that it would be necessary to change several PMOS transistor switches to full CMOS pass-gates. The use of single transistors in several areas of the circuit was originally favored because of the area savings, but with a single-ended power supply the PMOS gates can be held no lower than ground. The result is that a DC signal of roughly 800mV is needed on the input of the switch in order to pass a signal. This may be satisfactory when, for example, a signal is being applied for site impedance testing, and then being passed off the probe via the switch, or when site continuity mode is being used and a fairly large test signal can be passed through the continuity loop. If we desire to use the probe to compare buffered and unbuffered neural signals, however, it is not appropriate to use a PMOS switch because the neural signal is too close to ground and thus will not be passed. Using NMOS and PMOS transistors in parallel (with complementary gate inputs) will solve the problem, and this will be the approach taken in redesigning the probe.

During the coming quarter, these changes to the PIA-2B mask set will be completed. In addition, the modified mask set will include probes with an improved buffer, and a closed-loop amplifier. Design of these circuit blocks has been completed. Fabrication of the probes is expected to begin this quarter.

DC Stabilization of Electrode Systems

In order to accomplish the multiplexing of multiple neural channels onto a single output lead, it is necessary to achieve per-channel amplification of the neural signal. In this case, the DC offset of the site metal/electrolyte interface must be attenuated in order to accommodate the relatively high gain necessary without saturating the amplifier.

An I/V curve for a $100\mu m^2$ recording site is given in Fig. 9 below. This curve is based on data obtained experimentally for a $1cm^2$ site and adjusted for site area. A polynomial fit to the data is shown, and we can see that the open circuit potential of the site (relative to a Standard Calomel Electrode) is roughly 250mV. This is in agreement with other measurements. If we place a shunt device between the recording electrode and ground, then the intersection of the I/V curve of that device and the curve given in Fig. 9 will be the actual DC offset as seen at the amplifier input.

In the past, it has been suggested that a reverse-biased junction diode could be used as such a clamping device. This is illustrated schematically in Fig. 10. In this diagram, the open circuit (zero current) potential of the electrode is labeled Voc. The three diode curves represent the I/V curves for a diode under different conditions of illumination. The voltages V1, V2 and V3 represent the DC voltage at the amplifier input under these different conditions. It can be seen that such changes in the diode characteristics can lead to a tremendous variation in the DC offset. Changes to the diode I/V curve due to process variations have a similar effect. In fact, this is what was seen when a diode clamp was implemented, as reported by Qing Bai in her doctoral dissertation. What we desire, then, is a loading device with a load line which results in an intersection with the electrode I/V curve which is much less dependent upon illumination and process parameters.

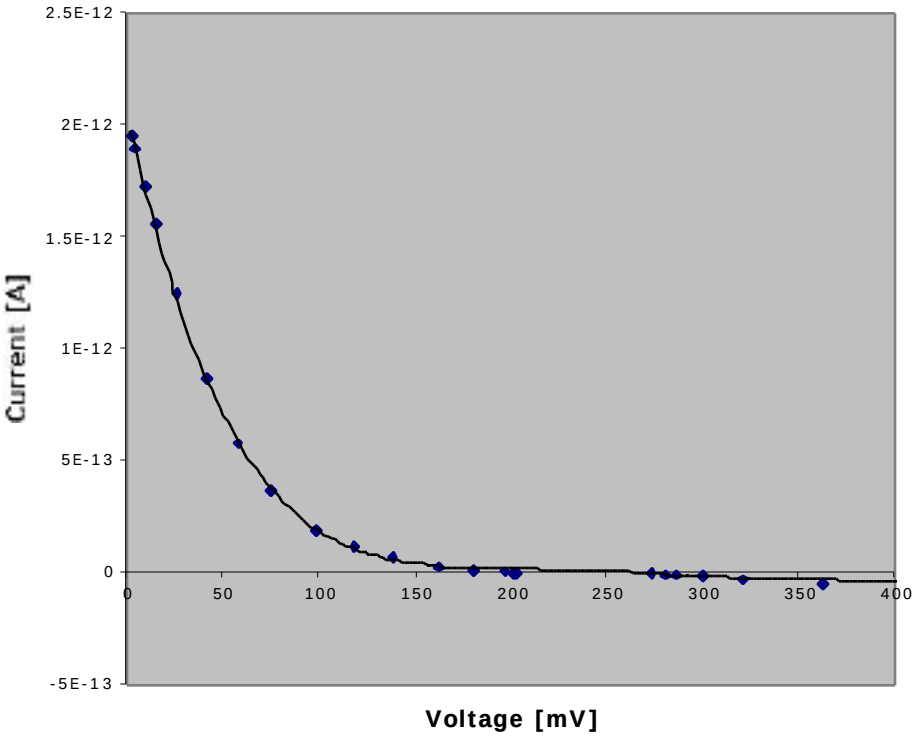

Fig 9: I/V Curve for 100μm^2 iridium site.

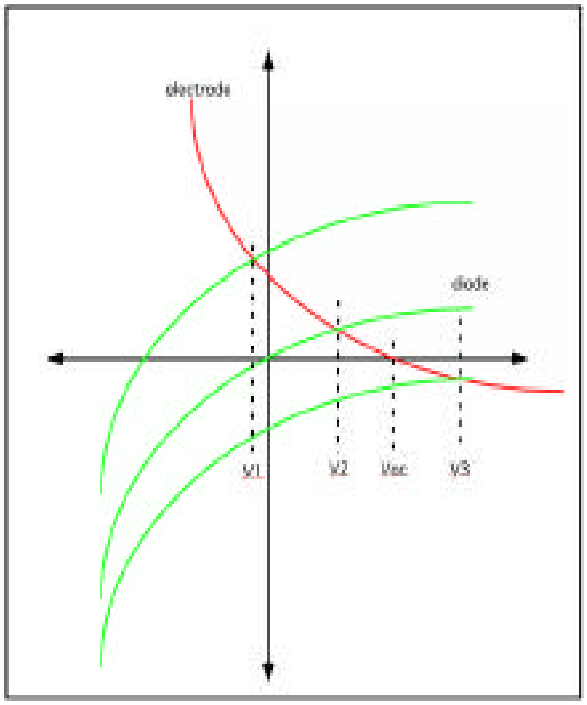

Fig. 10: Schematic load-line analysis for a diode-clamped electrode.

In past quarterly reports we have reported a method which uses a PMOS transistor biased in the subthreshold region as a clamping device. An amplifier clamped in this manner was fabricated at MOSIS, and excellent DC attenuation was achieved. Although measures were taken to reduce the susceptibility of the design to process parameter variations, it is yet to be seen whether this approach is sufficiently robust to be practical in the active probe process. Test structures and transistor-clamped probes will be included on an upcoming active probe run to answer this question.

During the past quarter, we have examined the use of arsenic-implanted polysilicon resistors for use in DC clamping. A test mask set was designed, and resistors were fabricated and tested. The resistors were fabricated in such a way that the additional processing could be merged with the existing active probe flow. Arsenic was chosen because it is relatively immobile during thermal processing, so that the resistance would be relatively stable even in the face of possible variations in subsequent thermal budget.

As shown in Fig. 11, the I/V curve of the resistors was very linear over a wide range of voltage (in this case 0 to 5 volts) and yielded sheet resistances of up to 35MΩ per square. This value could be increased by adjusting the target implant dose slightly. The light sensitivity of the resistors is clear from the figure, although it is important to note that the difference in illumination between the two curves is enormous. In the dark curve, the resistor was completely shielded from light, while in the light curve a microscope illuminator on the maximum setting was directed onto the resistor, corresponding to a luminant intensity of roughly 750 watts/cm^2 (of white light.) Note that in an actual probe situation, a metal shield would be used over the resistor to eliminate most light sensitivity.

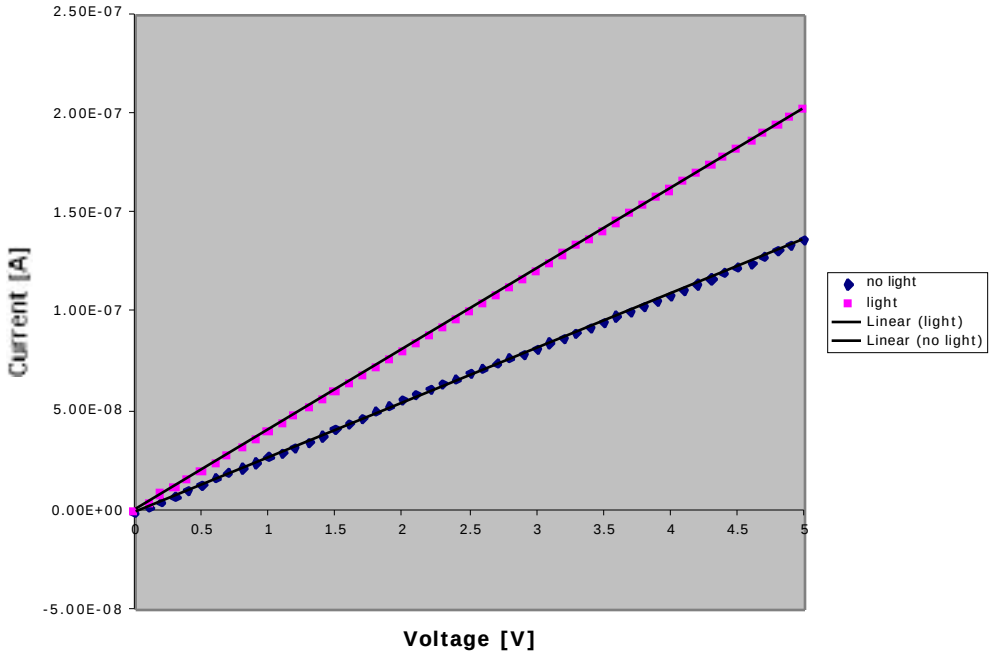

Fig. 11: I/V curve for a lightly-doped arsenic-implanted resistor. The inverse of the slope yields the resistance, in this case approximately 37MΩ for the dark case and 25 MΩ for the brightly illuminated case.

It can be seen from Fig. 11 that both curves cross relatively close to the origin, and that the illumination primarily affects the slope of the curve. Using linear regression, we can see that under the two extremes of illumination, the x intercept of the curves changes by only a few millivolts. This is different from the case illustrated in Fig. 10, where the nonlinear nature of the diode leads to very different axis crossings. The situation can be illustrated schematically in Fig. 12, where the changes in the resistor I/V curves due to illumination yield a relatively small change in clamped DC offset.

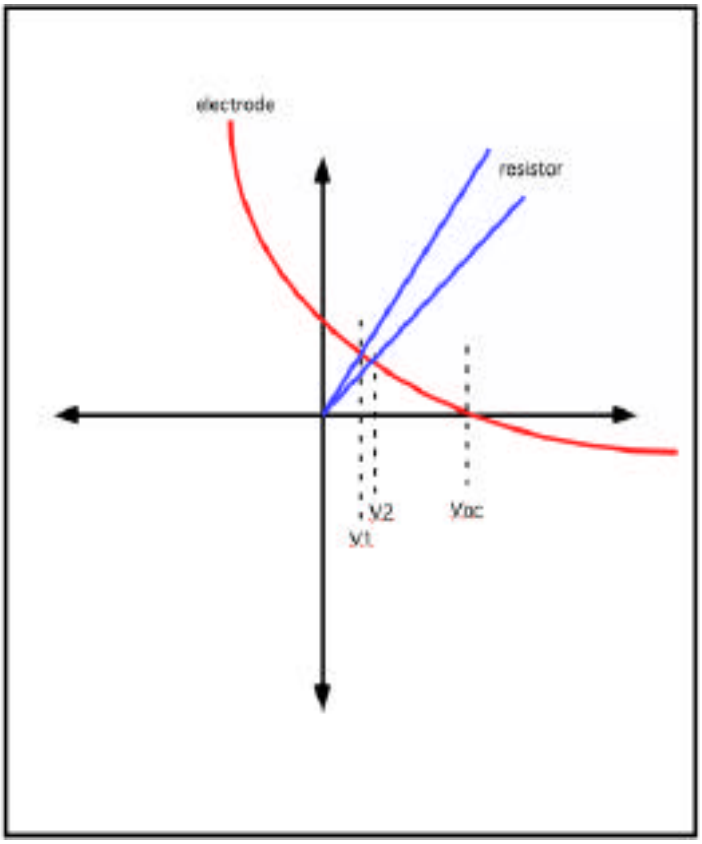

Fig. 12: Schematic load-line analysis for resistor clamped electrode.

In Fig. 13, the measured I/V curve of an arsenic-implanted resistor is plotted along with the measured I/V curve of an iridium electrode normalized for a 10,000μm^2 site. This is a huge site; it was chosen as an illustrative example because the data points are relatively scarce and it allows us to see the intersection of the curves. Here we see that the DC offset would be approximately 20mV; in the more realistic case of a 100μm^2 site this would be much smaller.

The results using an arsenic-implanted resistor so far have been encouraging. Further test wafers will be processed in the coming quarter to adjust the final sheet resistance and to evaluate run-to-run and across-wafer uniformity. In addition, in-vitro and in-vivo testing will be carried out using a probe with a diced resistor bonded on the PC board along with the probe. Integrated resistor clamps will also be included on the next active probe run for evaluation and comparison to the transistor clamps.

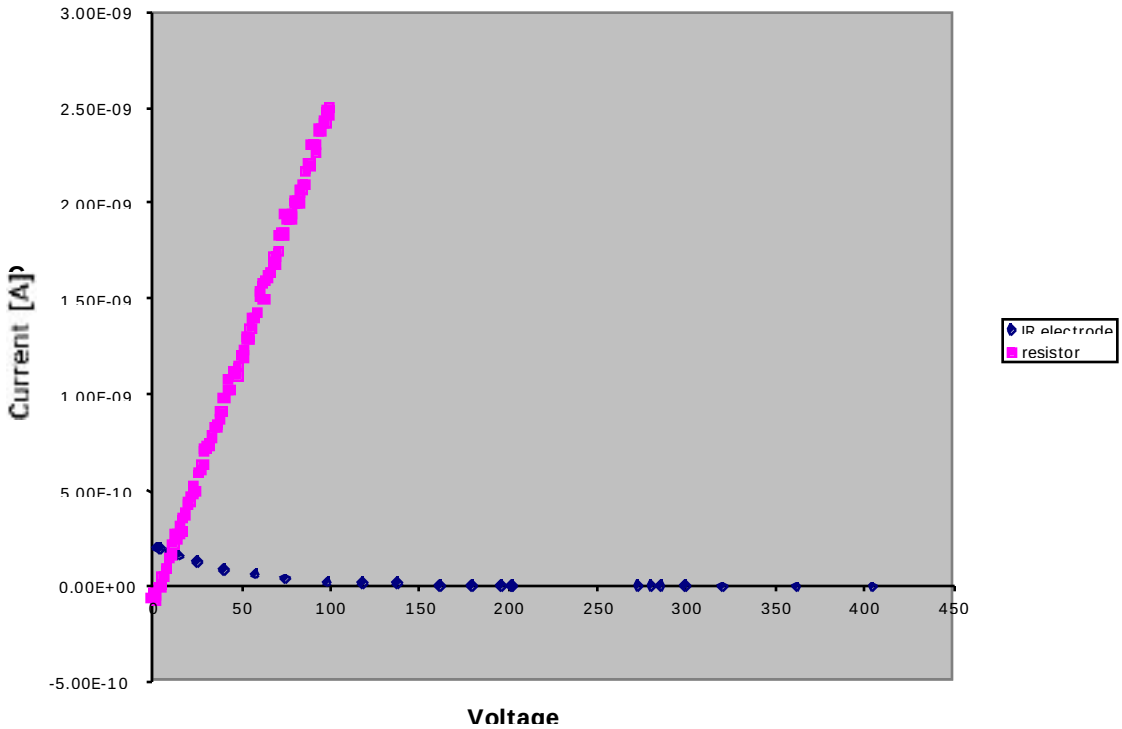

Fig. 13: Measured load-line analysis for resistor-clamped electrode.

Probe Design for Chronic Recording

During the past quarter, a mask set containing passive probes intended for chronic implantation has been developed. These probes will address questions regarding the nature of the tissue/electrode interface and the viability of long-term recordings. Specifically, we will explore the hypothesis that mechanical abrasion of sites due to small electrode movements contributes to longer periods of successful recording.

As shown in Fig. 14, these probes have sites which are likely to be exposed to small tissue movements due to their location either at the shank tip or overhanging the edge of the shank. The sites are located in close proximity to "standard" 177μm^2 sites, so that both types of site can record from the same neuron and comparisons of recording lifetime can be made. In a sense, the large tip site (roughly 1000μm^2) in the first probe above makes it a silicon microwire. This should provide a basis for a direct comparison of the chronic recording characteristics and life expectancy of the probe to that of microwires, which are widely used by the neuroscience community in chronic extracellular recording. The benefits of silicon neural probes for extracellular recording are numerous and have been enumerated elsewhere; however this type of comparison will be helpful in comparing the two types fo structures.

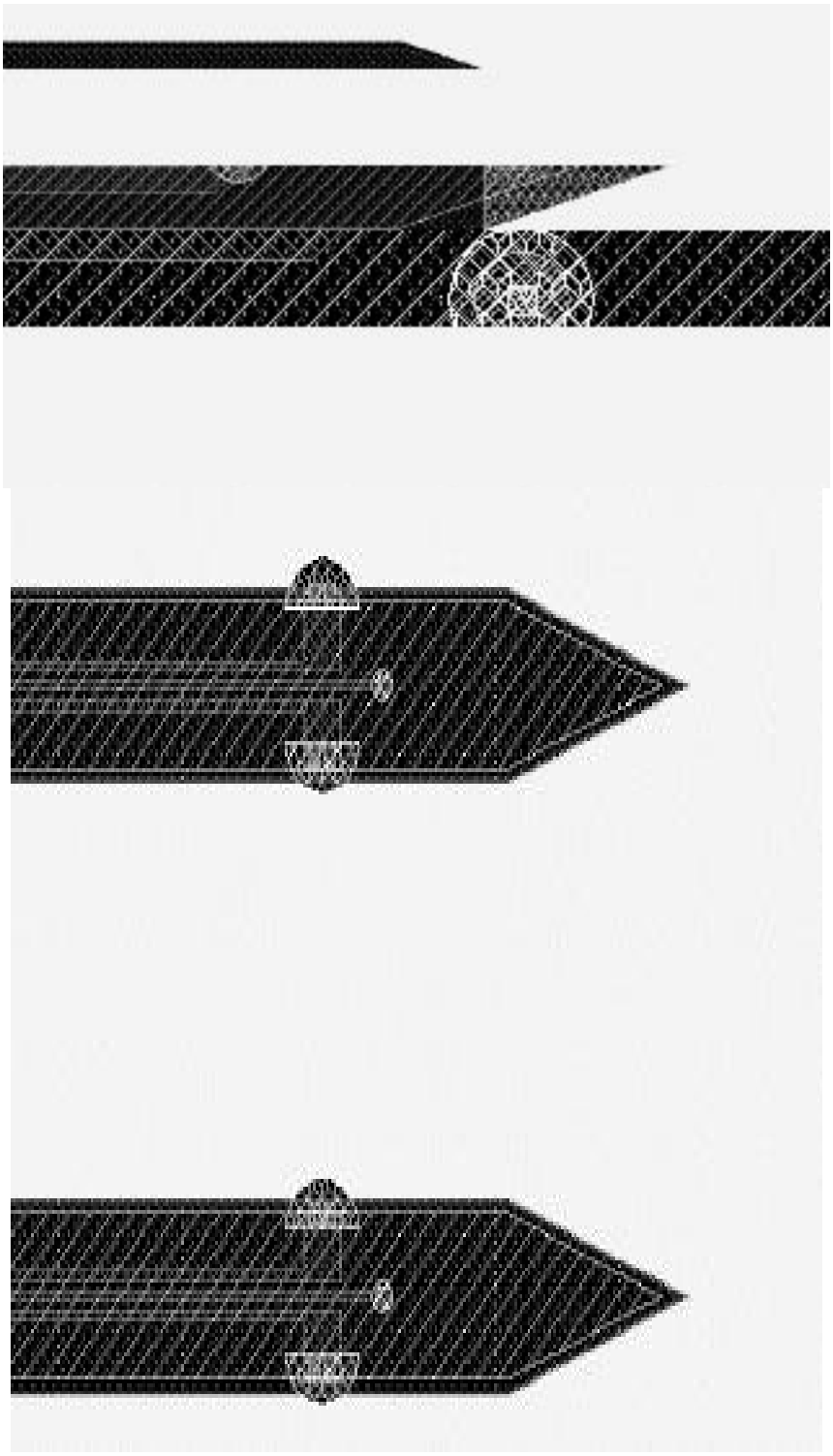

Fig. 14: Layout of the tips of chronic recording probes.

The probes are designed with integrated silicon ribbon cables which will be bonded to sixteen-channel Omnetics percutaneous connectors. Thus, these probes will provide a testbed for long term in-vivo testing of the silicon ribbon cables. In addition, the implants

will provide useful information about experimental procedure in chronic preparations. Fabrication of these probes will begin in the coming quarter, and it is hoped that a first cohort of chronic implants will be initiated as well.

5. Closed Loop Readout Amplifier Design for a Multiplexed Recording Probe

Due to the variable gains associated with the open-loop pre-amplifiers previously used on our recording probes, a closed-loop bandpass pre-amplifier has been developed. A schematic of the unbuffered amplifier can be seen in Fig. 15. The amplifier has a gain of 100 and a passband from 100Hz to 10kHz. Furthermore, the DC gain of the amplifier is near unity. The frequency response of the amplifier can be seen in Fig. 16. The total power consumption of the amplifier is 98.5µW from a ±1.5V supply. Eventually, when the amplifier is implemented an output buffer will have to be added to drive either a multiplexer or output leads. This output stage will be implemented using a push-pull output buffer to keep the power consumption to a minimum.

Due to the closed loop nature of the amplifier, it is much less susceptible to threshold shifts and other process variations than its open-loop counterpart. This amplifier in conjunction with either an input resistor clamp, or an input subthreshold biased MOSFET clamp, will form a second-order high-pass filter which should eliminate the problems associated with the varying DC potential at the electrode-electrolyte interface. A table listing the characteristics of the amplifier is presented below.

Gain	100
Pass Band	100Hz – 10KHz
Power Consumption	98.5 µWatts
Supply Voltage	±1.5Volts

Table 1. Closed Loop Pre-Amplifier Characteristics

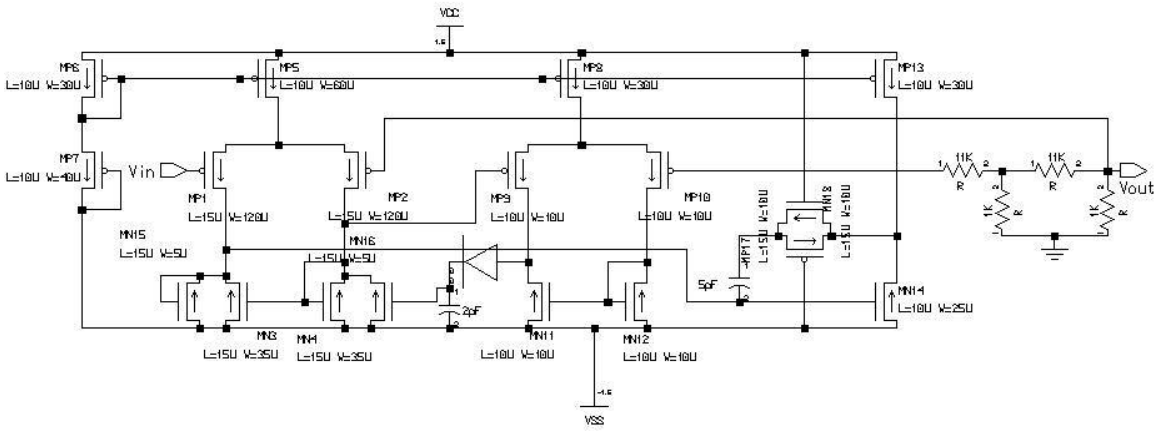

Fig. 15: Closed-Loop Amplifier Schematic

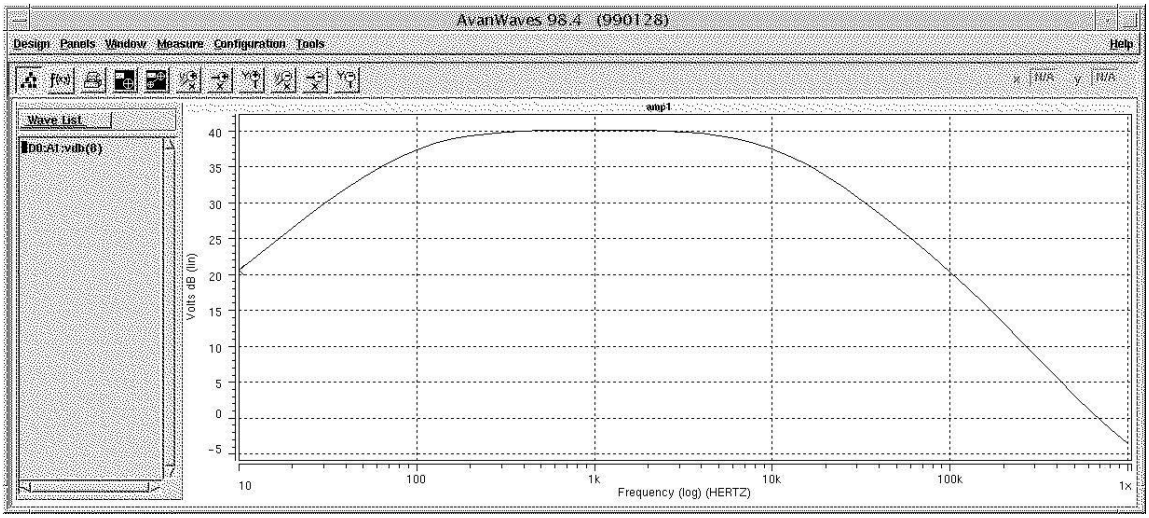

Fig. 16: Frequency response of the closed loop amplifier

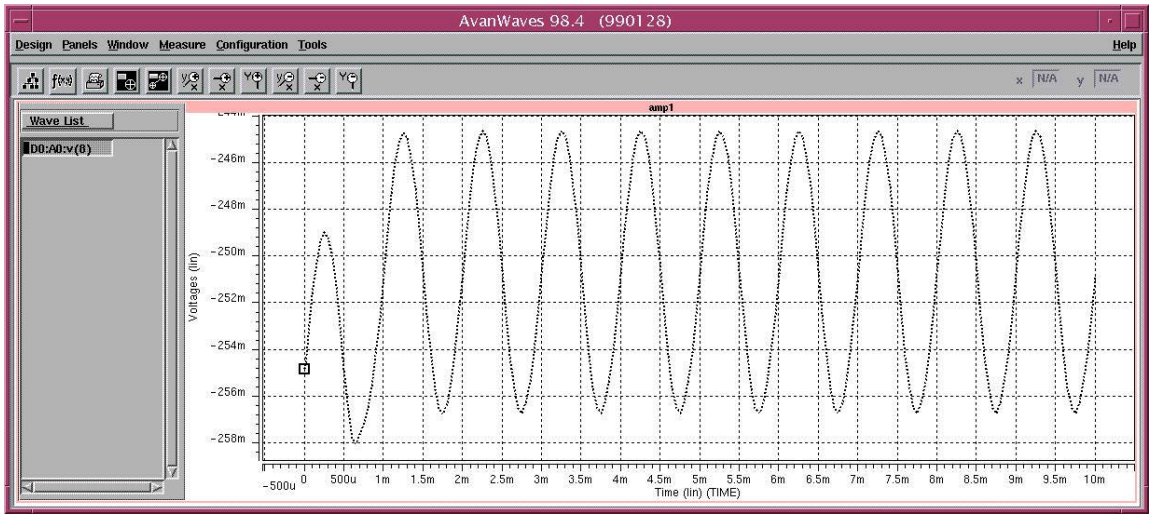

Fig. 17: Amplifier output with a 120µV p-p 1kHz sine wave input with no DC offset

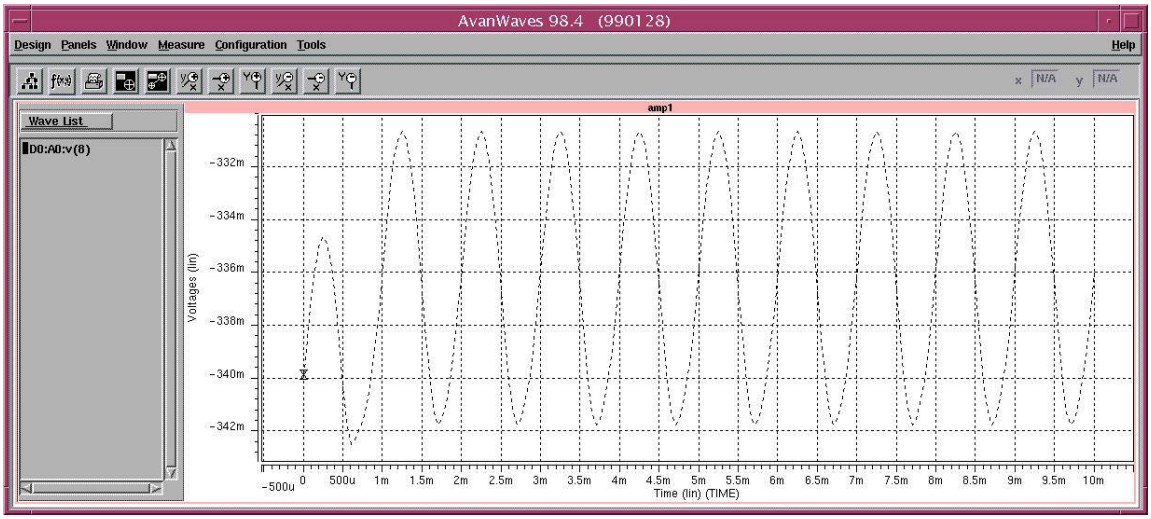

Fig.18: Amplifier output with a 120μV p-p 1kHz sine wave input having a 100mV DC offset.

6. Development of a Telemetry Interface for Wireless Probe Operation

6.1 Simulation and optimization of the circuit blocks of the telemetry system

During the past three months, research in this area has focused on reducing the power dissipation, improving the reliability of the circuits against threshold shift, and protecting the circuitry from large variations in the induced voltage. The details are discussed as follows:

1) Power on Reset and Clock Generator

The schematic and simulation results for the POR and clock circuitry were shown in the last quarterly report. The power dissipation of POR circuit becomes zero after finishing the power on reset, while the power dissipation of the clock generator circuitry is only 200μW. These circuit blocks are very simple so that their die areas are trivial.

2) Envelope detector

The schematic of the envelope detector circuitry is shown in Fig. 19, and the simulation waveform of this circuit is shown in Fig. 20. This circuitry is composed of a low-pass filter followed by a high-pass filter and Schmitt trigger. It can be easily seen that the cut-off frequency of LPF is determined by C2, MPlpf, MNlpf1 and MNlpf2. At the same time, the cut-off frequency of HPF is determined by C1, MPhpf1, MNhpf1. The frequency characteristic of LPF and HPF is shown in Fig. 21.

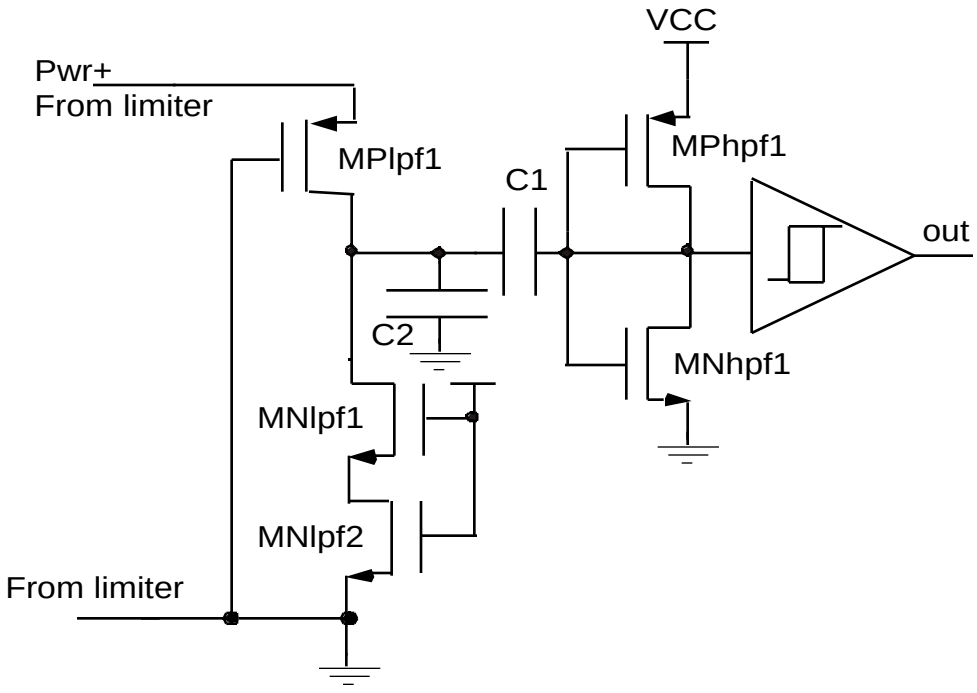

Fig 19: The schematic of envelope detector circuit

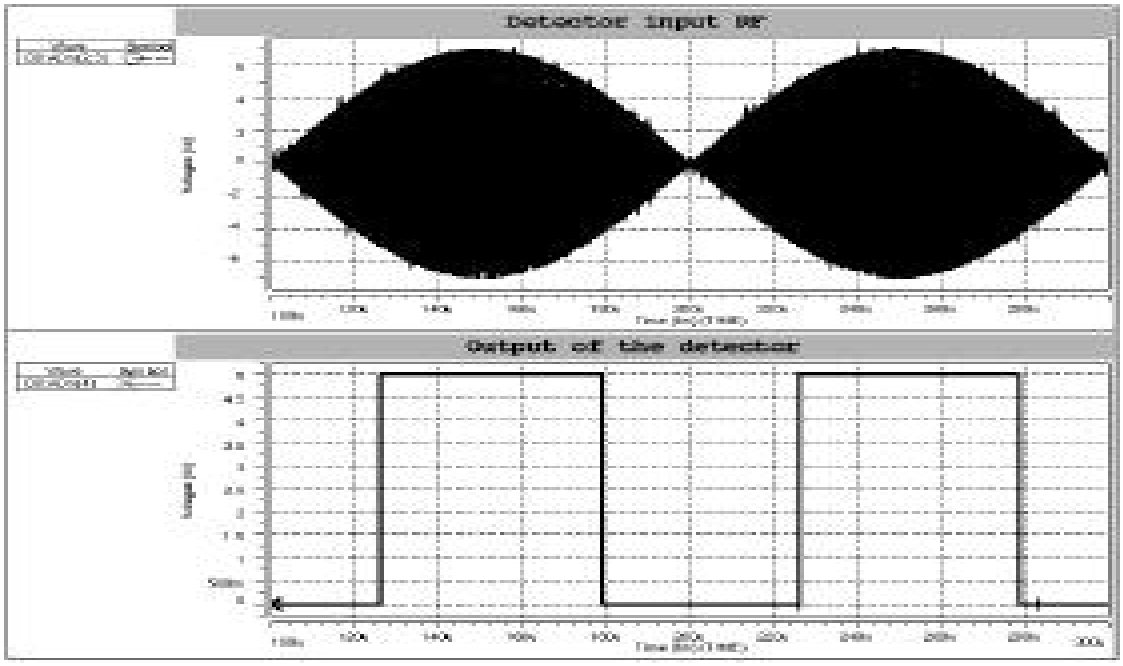

Fig 20: The simulation results for the envelope detector

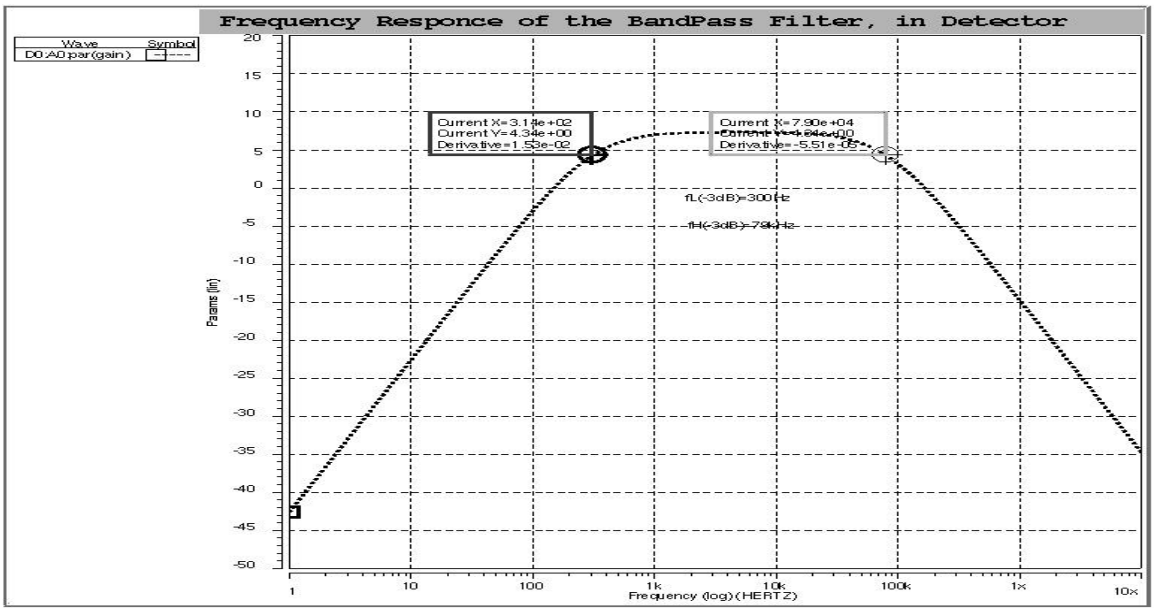

Fig 21: The frequency characteristic of LPF and HPF. f_H(-3dB)=79kHz, f_L(-3dB)=300Hz. The power dissipation of envelope detector is 300μW.

3) Voltage Regulator

The overall schematic of the voltage regulator is shown is Fig. 22, where bandgap circuit is shown in Fig. 23 and the startup op amp circuit are shown in Fig. 24.

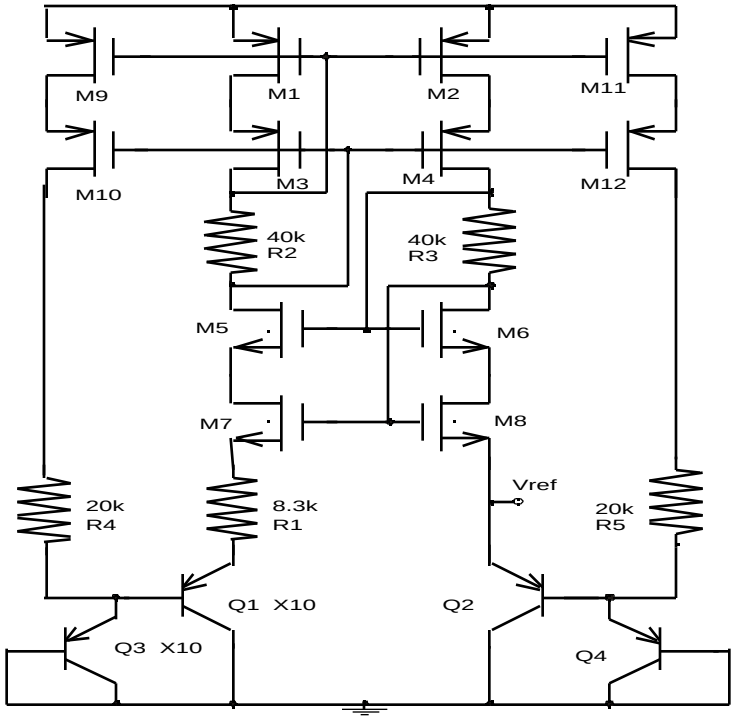

Fig. 22: The schematic of voltage regulator circuit

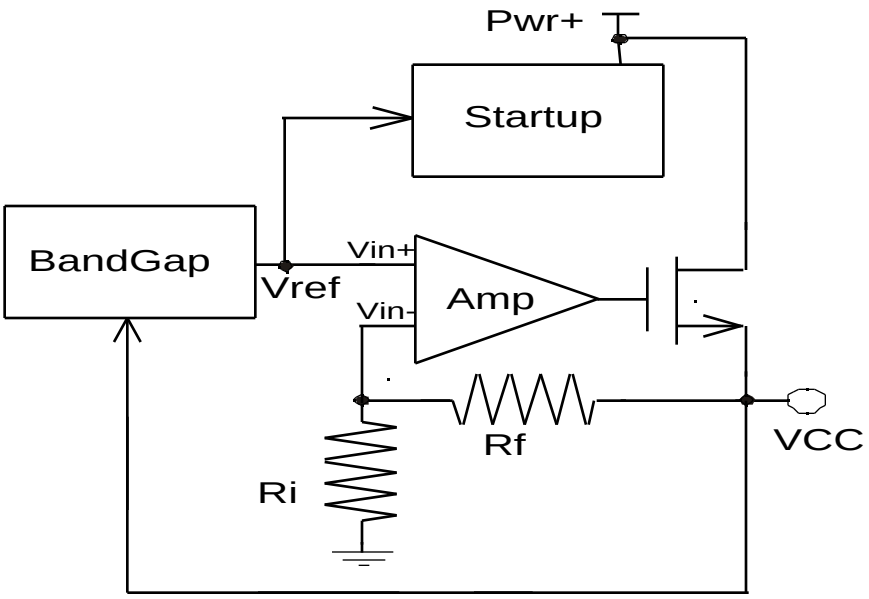

Fig. 23: Bandgap reference circuit

The bandgap voltage reference is used in this circuit in order to achieve good temperature independence and high power supply reject ratio. The reference voltage from bandgap is fairly stable even under large power supply variations.

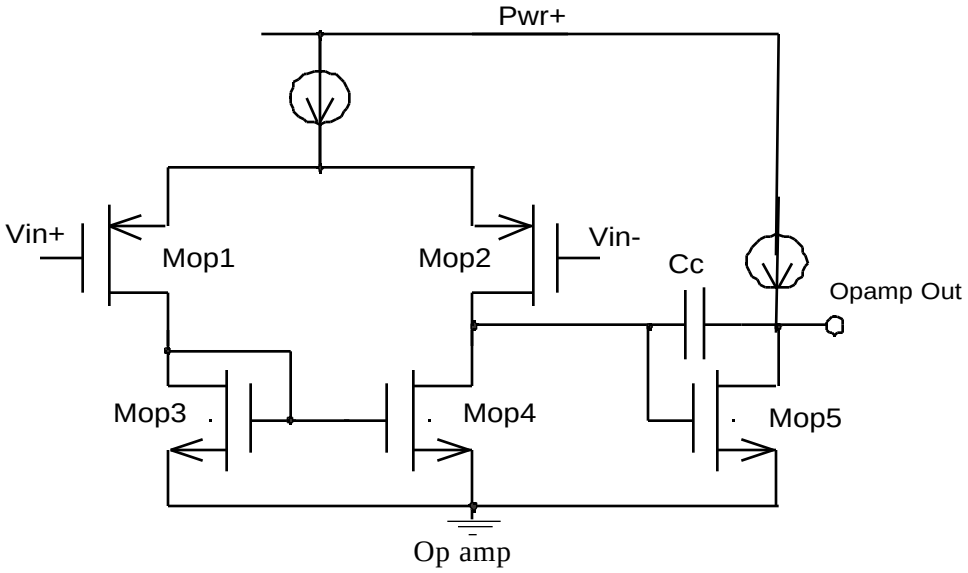

Fig. 24a: Schematic of the opamp circuit.

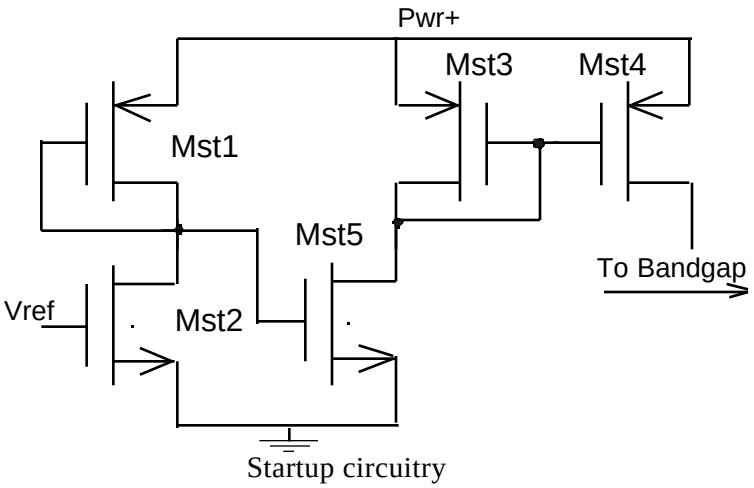

Fig. 24b: Schematic of the startup circuitry. The startup sub-circuit is included to drive the circuit out of its zero state, while the opamp, together with R_i and R_f, forms a feedback loop in order to stabilize the output voltage.

The simulation of the voltage regulator is plotted in Fig. 25. From the simulation results, we can see that the regulated output voltage is very stable, which satisfies the demands of the 10-bit ADC. For the input RF with the amplitude of 15V, the power dissipation of this circuit block is 4.2mW.

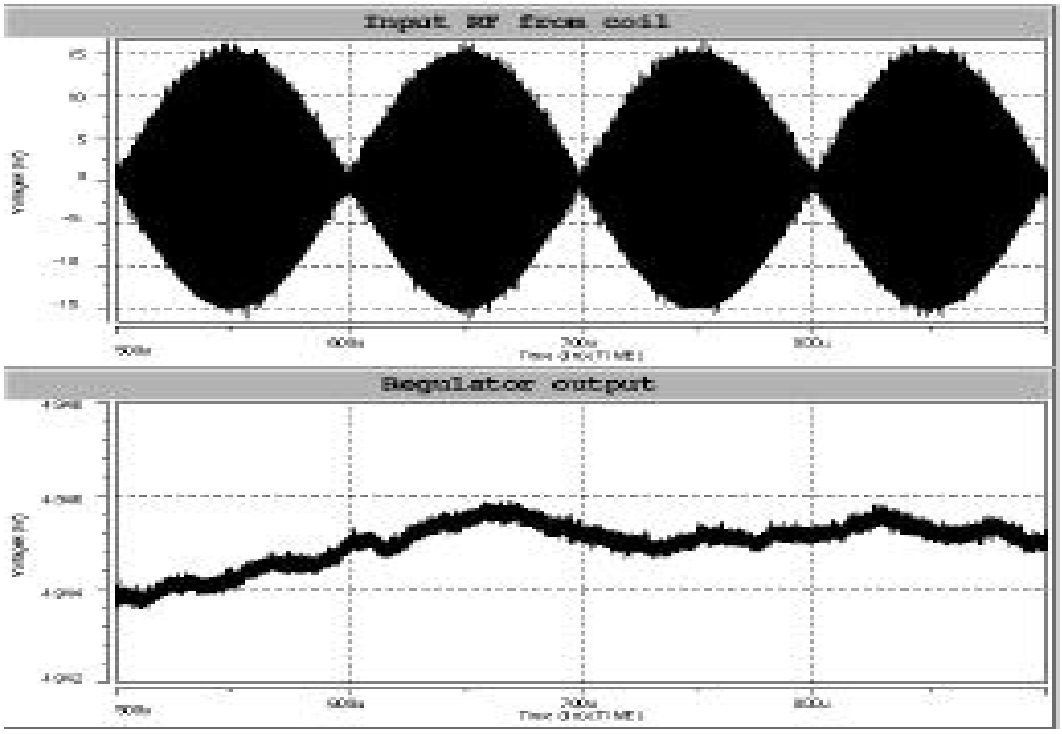

Fig. 25: Simulation results for the voltage regulator

4)_ RF Limiter

The distance between the external coil and internal telemetry may vary over a large range so that the induced voltage in the internal coil may change from several volts to several tens of volts. Because the breakdown voltage of the MOS transistor is limited, an RF limiter is used in this implementation to protect the telemetry. The schematic of RF limiter is shown in Fi. 26, and the simulation results are shown in Fig. 27.

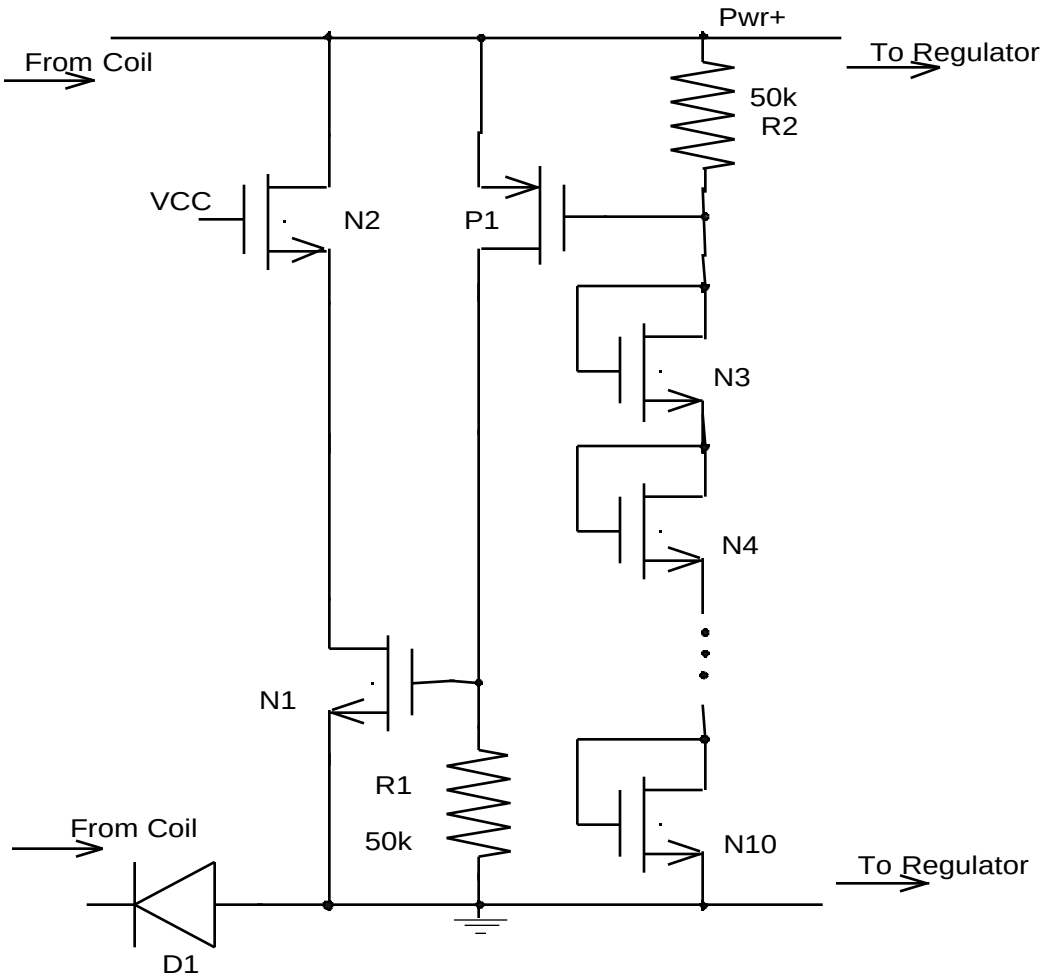

Fig. 26: Schematic of the RF limiter circuit

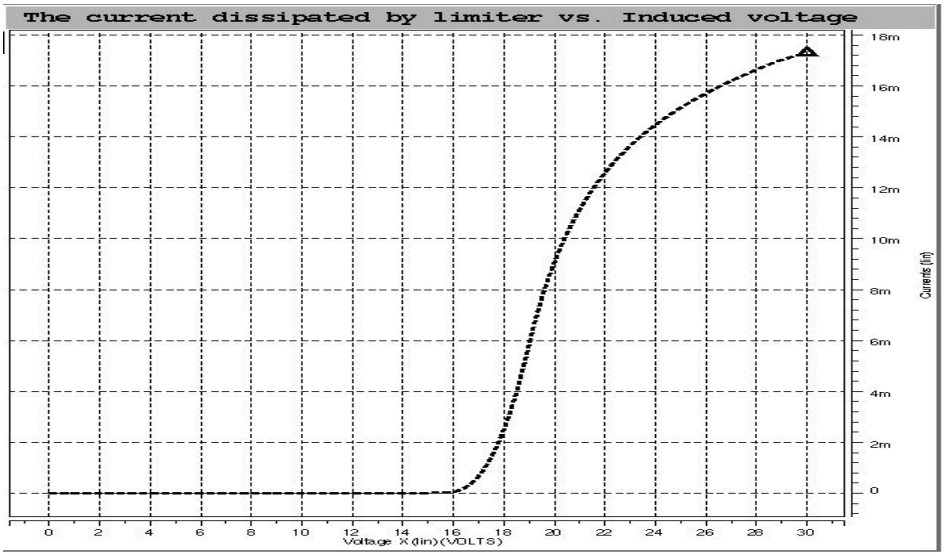

Fig. 27: Simulation results for the RF limiter circuitry

From the simulations, when the applied voltage exceeds 18V, the sinking current of the limiter increases quickly to more than 10mA so that it may confine the input current to the telemetry, thus protecting the telemetry circuit from high induced voltages. The power dissipation of the RF limiter, when input voltage is set to 15V, is 53μW.

All of the above simulations have been done under ±15% threshold voltage shifts; the circuit performance is still satisfactory in all cases. Simulations for all of the front-end circuit blocks together give us a power dissipation of 4.8mW for a sinusoidal input voltage with amplitude of 15V. Some important performance specifications and parameters are shown below:

Power dissipation (sinusoid input with amplitude of 15V)

Circuit block	**Power dissipation**
POR	0 (after power on)
Clock generator	0.2mW
Envelope detector	0.3mW
Regulator	4.2mW
RF limiter	0.05mW
Total	4.8mW

Some important parameters

Parameter	**Specification**
Power on reset pulse width	18μs
Detector Higher cut-off frequency	79kHz
Detector Lower cut-off frequency	300Hz
Detector trigger amplitude	4.5V(rise), 4.1V(fall)
Clock frequency	4MHz
Regulator output voltage	4.943-4.946V

Circuit Layouts

The AMI ABN (1.5µm) process was chosen for the implementation of the telemetry circuits using the MOSIS foundry. A lambda of 0.8µm for the AMI ABN process is recommended by MOSIS to improve consistent and uniform electrical behavior for both analog and digital designs. The MOSIS ABN process offers two metals, two polysilicon levels, and an optional BJT NPN. Two poly layers are used to implement capacitors, and a P-base optional layer is used for any NPN transistors. In addition, substrate PNP transistors are implemented for the bandgap circuitry. The diodes in the half-rectifier are realized by the junctions between the p-substrate and the n-well. A lot of test devices were included in this layout in order to obtain some critical circuit parameters for further improvement. The layout of the whole circuit is shown in Fig. 28.

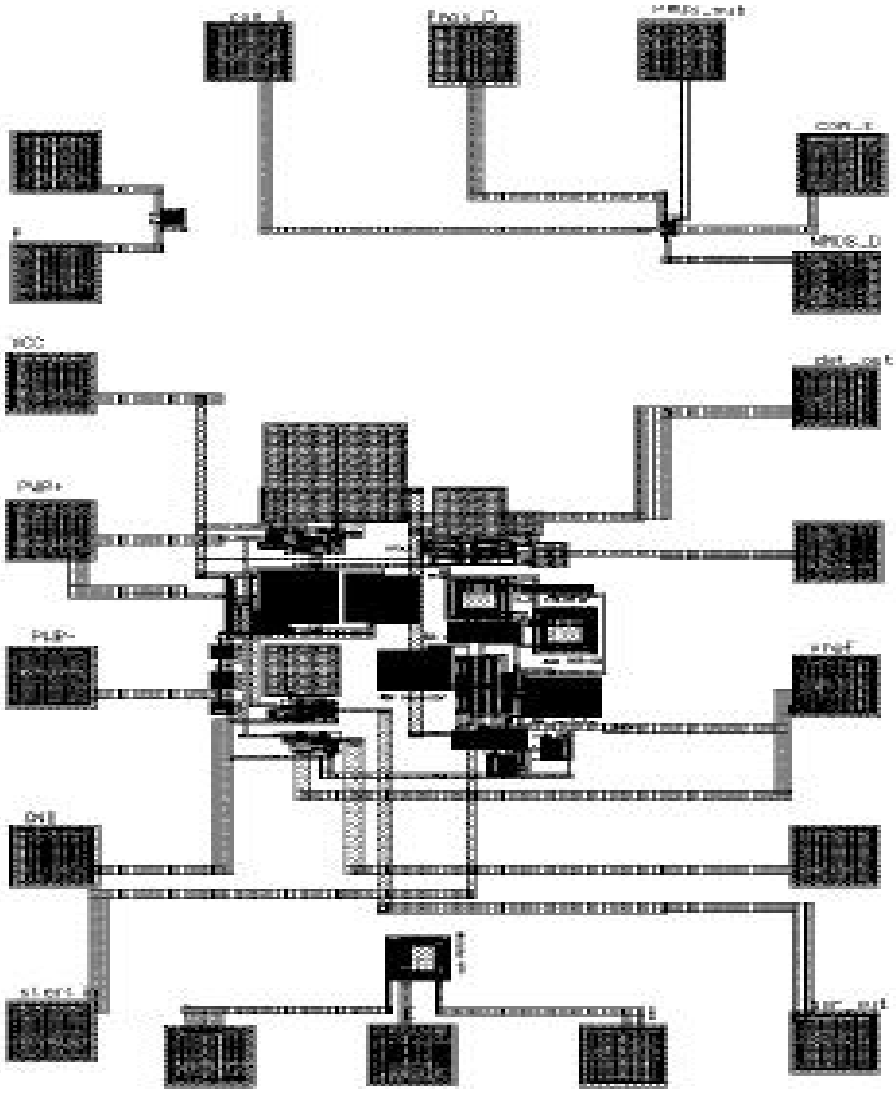

Fig. 28: Layout of the front-end telemetry circuits

5. Conclusions

During the past term, we have continued to fabricate additional passive probes for use by a variety of investigators. This has included processing additional wafers of our standard probe designs as well as designing two new mask sets of custom designs. The second of these will employ 1.5μm features, shrinking current dimensions by a factor of two. We have also implanted passive probes in guinea pig inferior colliculus and auditory cortex using normal and side-mounted recording sites. The standard sites have typically recorded for about one month, while the side mounted sites are still recording after three weeks as of this writing. We expect the side-mounted sites to do better since micromovements there will tend to clear the sites of protein layers that are hypothesized to mask recorded units from the site surface. We have found that by inducing brain movement by hyperventilating the animals successfully and repeatedly restores recording ability. This will be explored further. Polypyrrole is being explored as a recording site material because this polymer can be doped to prevent the adhesion of protein on its surface. These sites are low in impedance but have experienced some adhesion problems which are being addressed. We hope to have longer-term recording experiments with polyprrole to report by the end of the coming quarter. We have also developed improved cleaning procedures for use on probes destined for chronic use. Experiments in culture medium with bovine serum have shown that without the new cleaning procedures, adverse cell reactions and cell death in the immediate vicinity of the probe surface sometimes occur.

A series of passive probes have been designed to allow a direct comparison with microwire electrodes and are now being fabricated. The design of our non-multiplexed active recording probe, PIA-2B, is now being iterated to upgrade its switches and recording buffers. A resistor technology based on ion-implanted polysilicon has been developed to allow simple resistive input clamps to be used to stabilize the input bias of the preamplifiers by loading down the electrochemical cell formed at the recording site. As presented previously, we require an input dc resistance between about 75MΩ and 500MΩ in order to achieve proper stability in the face of both battery offsets and optically-based current generation. The resistor technology allows a sheet resistance of 35MΩ/square to be achieved, so that such resistances would require very little area at the preamplifier inputs and would stabilize the input dc levels to better than 1mV in the face of several hundred millivolt offsets. Finally, we are continuing to refine designs for closed-loop preamplifiers and for the various circuits required for the realization of a telemetry-based probe interface. We hope to include the new preamplifiers on the modified version of PIA-2B as well as on a redesigned version of PIA-2/-3 that is now in development.